

Requirements on common solutions to the LSND and MiniBooNE excesses: a post-MicroBooNE study

Waleed Abdallah,^a Raj Gandhi^b and Samiran Roy^c

^a*Department of Mathematics, Faculty of Science, Cairo University, Giza 12613, Egypt*

^b*Harish-Chandra Research Institute (A CI of the Homi Bhabha National Institute), Chhatnag Road, Jhansi, Allahabad 211019, India*

^c*Institute of Physics, Sachivalaya Marg, Sainik School Post, Bhubaneswar 751005, India*

E-mail: awaleed@sci.cu.edu.eg, raj@hri.res.in, samiran.roy@iopb.res.in

ABSTRACT: The strong statistical significance of an observed electron-like event excess in the MiniBooNE (MB) experiment, along with an earlier similar excess seen in the Liquid Scintillator Neutrino Detector (LSND), when interpreted in conjunction with recent MicroBooNE results may have brought us to the cusp of new physics discoveries. This has led to many attempts to understand these observations, both for each experiment individually and in conjunction, via physics beyond the Standard Model (SM). We provide an overview of the current situation, and discuss three major categories under which the many proposals for new physics fall. The possibility that the same new, non-oscillation physics explains both anomalies leads to new restrictions and requirements. An important class of such common solutions, which we focus on in this work, consists of a heavy $\mathcal{O}(\text{MeV} - \text{sub-GeV})$ sterile neutral fermion produced in the detectors, (via up-scattering of the incoming muon neutrinos), and subsequently decaying to photons or e^+e^- pairs which mimic the observed signals. Such solutions are subject to strong demands from a) cross section requirements which would yield a sufficient number of total events in both LSND and MB, b) requirements imposed by the measured energy and angular distributions in both experiments and finally, c) consistency and compatibility of the new physics model and its particle content with other bounds from a diverse swathe of particle physics experiments. We find that these criteria often pull proposed solutions in different directions, and stringently limit the viable set of proposals which could resolve both anomalies. Our conclusions are relevant for both the general search for new physics and for the ongoing observations and analyses of the MicroBooNE experiment.

KEYWORDS: LSND excess, MiniBooNE excess, MicroBooNE

Contents

1	Introduction	1
2	The LEE and its resolution via new physics: a post-MicroBooNE overview	3
3	The up-scattering interaction, cross section and event rate	7
4	Requirements resulting from the variation of the cross section with incoming neutrino energy and with mediator mass	9
5	Requirements resulting from fitting the angular distribution in MB	11
6	Requirements resulting from considerations related to the energy distributions in LSND and MB	14
7	Requirements resulting from considerations related to the visible signal in LSND and MB	16
8	Discussion	17
9	Conclusions	18

1 Introduction

The observation of unexplained electron-like excesses in the Liquid Scintillator Neutrino Detector (LSND) [1] and the MiniBooNE (MB) experiment [2–4] has provided an important window of opportunity in our search for physics beyond the Standard Model (SM). This importance is based on the strong statistical significance of these excesses (3.8σ for LSND [5] and 4.8σ for MB [4], with a combined significance of 6.1σ [3]). The results are buttressed by careful estimates and measurements of possible SM backgrounds in order to eliminate standard physics explanations. (For discussions, see *e.g.* [6–11] and references therein.)

Both experiments differed in beam energy by an order of magnitude, and had very different systematic uncertainties and backgrounds, implying that if indeed standard physics was responsible for the excesses observed, it would likely require two qualitatively different explanations. While MB confirmed the presence of an electron-like excess in the low-energy region of its range in its effort to validate the LSND observations, both LSND and MB were insensitive to whether the excess originated in electrons, photons or collimated e^+e^- pairs¹. The MB neutrino fluxes peak around 800 MeV while the energy of the primary

¹In what follows, we use the acronym “LEE” (for low energy excess) to refer to both the LSND and the MB excesses, although in the literature for the most part it is used for the MB excess only.

decay-at-rest (DAR) flux ($\bar{\nu}_\mu$) of LSND was significantly lower, going down to as low as ~ 50 MeV. LSND also had a decay-in-flight (DIF) flux, going up to ~ 250 MeV.

Very recently, the MicroBooNE experiment [12], designed specifically to be sensitive to differences between the various signal possibilities mentioned above and help pin down the origin of these anomalies, announced its first set of results [11, 13–16], which seem to offer further support for the presence of new physics. A major goal of the experiment is to search for an LEE signal in ν_e charged-current (CC) interactions with an electron in the final state (the eLEE search) as well as in neutral-current (NC) interactions with a single photon in the final state. Four separate searches and analyses were carried out: i) a final state photon produced by Δ production and decay; ii) an exclusive search using the charge current quasi-elastic (CCQE) interaction channel; iii) a semi-inclusive search for events with one electron and no final state pions; and iv) a fully inclusive search for events with one electron and any other possible final state. MicroBooNE expected, but did not see, any excess in electrons beyond SM backgrounds. Their results thus so far indicate that the MB excess was not due to electrons. Moreover, the most likely photon-producing SM background (i) above) was measured to be consistent with expectations.

We note that these results are based on a part (6.8×10^{20} protons on target) of what will eventually comprise the full MicroBooNE data sample, and may change with further data and analysis. However, in spite of the fact that MicroBooNE saw results in conformity with the SM, at the present time these seem to point (albeit not unequivocally) to the possibility that the excess could stem from a) single photons or b) the production of e^+e^- pairs, with their origin lying in new physics. This conclusion is based upon the following reasoning:

- It is assumed that the MB LEE is *robust*. This assumption is based on (a) data-driven background measurements, (b) comparisons with state-of-the-art neutrino generators and (c) estimates of theoretical uncertainties, as discussed in [7, 9] and references therein.
- By confirming that the largest and most likely single photon background is in conformity with production rates dictated by the SM [11], MicroBooNE has pointed out that if the LEE is due to photons, they are likely produced via new physics arising from mechanisms like radiative decay of heavy neutrals and/or non-standard magnetic moments. This conclusion is to be drawn in juxtaposition with MB’s own measurements of control samples of single photons from π_0 production and decay, and from Δ (1232) production and decay [17].
- As mentioned above, via three searches for ν_e scattering leading to the production of electrons [13–16], each with a different final state, MicroBooNE excluded an electron final state parametrisation of the MB excess (the eLEE model) at a confidence level $> 97\%$. By doing so it disfavoured (but did not eliminate) the possibility that the excess originated in sterile-active neutrino oscillations and strengthened the possibility that the excess could be due to boosted e^+e^- pairs, which, not having a known SM background, points to new physics.

Given the potential for discovery, it is important to examine aspects of the possible new physics scenarios and their implications. We attempt to do this by first providing an overview of the present situation as it stands post the MicroBooNE results in section 2. The rest of our paper is focussed on studying an important class of new physics solutions which will soon be tested by MicroBooNE and subsequent experiments. Specifically, we study, from a phenomenological perspective, the demands placed on non-oscillation new physics which attempts to explain both these anomalies simultaneously. We restrict ourselves to a class of solutions where a new heavy sterile neutrino is produced inside either detector (LSND or MB), via up-scattering of the incoming beam ν_μ (or $\bar{\nu}_\mu$), and which subsequently decays in a manner that mimics the observed signal for the excess by producing an e^+e^- pair or a photon. This final state is produced by new fermions and/or boson mediators [18–30]. We find that once one fits MB, important restrictions ensue on demanding that the same benchmark parameters also explain LSND, narrowing and illuminating the search for new physics. The conclusions we obtain are also relevant to observations and analyses focussed on new physics currently in progress in the MicroBooNE experiment.

Section 3 describes the up-scattering interaction in the detector and provides expressions for the cross section and event rate. Section 4 focusses on the variation of the cross section with incoming neutrino energy for two different types of mediators (neutral vectors and CP-even scalars)² and also examines the behaviour of the cross section with different mediator masses. In section 5 we study the requirements imposed by fitting the MB angular distribution. Section 6 examines information that can be obtained by studying the energy distributions in both detectors, while section 7 studies the kinematics of decay of the up-scattered heavy neutrino and its effect on the requirements. Section 8 collates the information in sections 2–7 to arrive at a set of final requirements on a common solution. Finally, section 9 summarizes our conclusions.

2 The LEE and its resolution via new physics: a post-MicroBooNE overview

If one were to classify the many new physics proposals³ made to understand the LEE keeping the recent MicroBooNE results in mind, one finds that most of these fall under one of three broad categories **a)**, **b)** or **c)** below, depending on the final state they produce in these detectors⁴. This classification is convenient because of MicroBooNE’s ability to distinguish among them:

- a) Proposed solutions in this category are distinguished by the fact that their final state, both in LSND and MB is a *single electron or positron*. Since the announcements of the LSND and subsequently, the MB results, much attention over the past decade or more has been focussed on light sterile neutrinos of mass $\mathcal{O}(\text{eV})$, with consequent active-sterile mixing and oscillations to ν_e or $\bar{\nu}_e$ to account for the observed signals. We

²Hereafter, we simply refer to these two mediators as vector and scalar mediators.

³These include proposals that attempt to explain one or the other anomaly, or both simultaneously.

⁴Some proposals cannot be classified easily within the simple scheme we have chosen here, since they combine two of the three final states, *e.g.* [28–30].

note that in addition to LSND and MB, other short baseline experiments at nuclear reactors [31], and radioactive source experiments [32, 33] have reported anomalous signals involving electron neutrinos. The picture regarding their inter-connectedness to LSND and MB, however, remains unclear. Recent reviews and references on active-sterile oscillation solutions to the anomalies may be found in [8, 34–38]. Variants on the simple vacuum oscillation solution, which use matter effects and resonant oscillations with new mediators to produce a single electron or positron in the detector may be found in [39] (vector mediator) and [40] (scalar mediator).

A second subset of solutions, which fall into this category because they produce the same final state, but are distinct from the point of view of the physics involved, invoke the production of additional ν_e (or $\bar{\nu}_e$) in the beam. These ν_e have their origin in the decay of a heavy neutrino (ν_4 , eV to hundreds of keV in mass) to mostly-active neutrinos via $\nu_4 \rightarrow \nu_i + \phi$, where ϕ is a new scalar and ν_i an SM neutrino [41–45].

Both subsets of proposals in category **a)** remain in contention due to reasons described in recent work [39, 46–48], *i.e.* that MicroBooNE results disfavour but do not eliminate the possibility that LSND and MB results can be explained by i) $\mathcal{O}(\text{eV})$ sterile neutrinos with active-sterile mixing and oscillations, or more generally, by ii) the presence of additional ν_e in the beam. Arguments about the viability of these choices draw upon a reanalysis [46] of the MicroBooNE data viewed in conjunction with other indicators of active-sterile oscillations, like the source experiments (SAGE, GALLEX and BEST [32, 33]) and the reactor flux calculations and data [31, 49, 50]⁵. They also assign weightage to the systematic uncertainties present in the backgrounds at MB. Importantly, they rely on the fact that MicroBooNE mapped the MB excess to an eLEE model which is not unique, in that other ν_e spectral choices can also reproduce the MB excess [39, 47]. These considerations render MicroBooNE’s coverage of MB’s parameter space less certain and extensive, and consequently do not rule out these proposals.

- b)** A second category of proposals proceeds on the basis that i) the conflict with ν_μ disappearance data (discussed below), ii) the tension with cosmology (below), iii) the apparent discrepancy between the oscillation parameter space identified by source experiments and reactor data [51] along with iv) the recent MicroBooNE results, when considered in conjunction, constitute sufficient evidence that while heavier sterile neutrinos might well be part of nature’s particle spectrum, they do not seem to reside in the mass and mixing parameter space singled out by oscillation explanations of the various low energy anomalies discussed above. The final state in these proposals is not a single electron or positron, but *an* e^+e^- pair produced in the detector [18–25, 27–30, 52]. The focus is on finding other explanations involving new physics in production and decay for the LSND⁶ and MB anomalies. Many such proposals postulate a new

⁵We note that recent improved calculations [51] of inverse beta decay yields at reactors appear to disfavour the existence of a reactor anomaly and point to a significant tension with the parameter space identified by the Gallium source experiments, making the link between the two tenuous.

⁶LSND did not conduct a search for e^+e^- pairs or $\gamma\gamma$ pairs. Due to this reason it is reasonable to assume that it would reconstruct most e^+e^- pairs as a single electron event. Specifically, since timing was their

physics interaction involving a vector or scalar mediator which is not part of the SM spectrum, as well as heavy sterile neutrinos, several orders of magnitude higher in mass than those in the oscillation scenarios of category **a**).

- c)** A third category of proposals has, as a final state, a single photon which could have its origin in either production via coherent nucleus scattering [53, 54], or an anomalous magnetic moment [25, 26], or other new physics process occurring in the detector involving a photon as a decay product [27–29, 55]. These are also based on the assumptions **i)–iv)** as in category **b)** above.

All of the proposals listed above are subject to strong and multiple constraints, which is expected given the low energies involved, the solidity of the SM and the multiplicity of experiments which have tested it over five decades. Indeed, it has been shown that many of the proposals are disfavoured or in significant tension with data. To embark on a discussion of all possible bounds on them and their ramifications is beyond the scope of our paper and of our aim in this section, but we briefly mention some important classes of constraints below along with some relevant references:

- With respect to the sterile-active oscillation proposals in category **a)** above, it has become evident over time that sterile neutrinos which can account for appearance data in short baseline experiments like LSND and MB are in very significant tension with ν_μ disappearance data. Additionally, such neutrinos, which only interact due to mixing with SM neutrinos, must contend with stiff constraints from cosmological data [56–58]. For a discussion and complete references for this very active field, the reader is referred to the review articles [8, 59–63].
- The other sub-category of solutions in category **a)** which lead to additional ν_e in the beam due to heavy neutrino decay, introduce new interacting states. In many cases, such states affect and can be tested against cosmological observations, such as primordial nucleosynthesis yields and the total amount of energy density carried by neutrinos at late times. They can also be constrained by considerations of the supernovae neutrino spectra and the existing bounds on the flux of antineutrinos from the sun, and from event rates measured at near detectors of many accelerator-based neutrino experiments. For a discussion and references, see [64, 65].
- Proposals in category **b)** are subject to multiple constraints, from near detectors in neutrino experiments, meson decay data, high and ultra-high energy neutrino experiments, colliders, active-sterile mixings, beam dump and dark photon searches, among others. Discussions and references may be found in [24, 55, 64, 66–77].
- Proposed solutions to the anomalies which belong to category **c)**, *i.e.* where a new physics interaction produces a photon in the final state share many of the same

most powerful particle identifying variable, the fit to a Cherenkov ring would automatically select the most significant ring, even for large angles between the e^+e^- pair. For this reason, e^+e^- pairs with correlated neutrons could explain the LSND excess.

constraints related to mixings between active and heavy sterile neutrinos [55, 66–70, 75, 77], since the photon production in many cases is via radiative decay of a heavy neutral lepton. In addition, anomalous magnetic moment constraints [55, 78–80] may be applicable. In some cases the produced photon is excessively forward, hence is constrained by the observed angular distribution at MB [81].

The new physics proposals in all three aforementioned categories can be tested rigorously in the near future by the Fermilab Short Baseline Neutrino (SBN) program, comprising of three Liquid Argon Time Projection Chambers (LArTPCs) [82] set along the booster neutrino beam at different baselines. These will allow definitive tests of the sterile-active hypothesis (discussed in category **a**) above). In addition, their excellent capability to collect ionization electrons from charged particles passing through the argon in the LArTPC will enable detailed track reconstruction, measurements of deposited energy and particle identification for all three types of final states characterizing the new physics proposals.

Overall, at this point in time, it is reasonable to state that the case for new physics arising from an understanding of the LSND, MB and now MicroBooNE results is strong, as opposed to the case for the results being due to SM backgrounds or systematic errors. While SM explanations of the excesses are possible, we note that since the first reports of an excess in LSND about 25 years ago, almost every new result from these experiments, whether it has been a measurement or an estimate of an important SM background or the gradual accumulation of evidence for the excess observed, has strengthened, not weakened the case for new physics. Such physics may lie among the many proposals covered by categories **a**), **b**) and **c**) above, or could be some as yet unimagined new possibility.

If, indeed, the excesses are due to new physics, it is difficult to over-estimate the import and breadth of the consequences that would ensue. We make a brief (and incomplete) attempt to give some idea of their range and impact by listing the physics consequences of some of the proposals listed above:

- A 4.6σ discrepancy between early-universe and late-universe measurements of the Hubble parameter H_0 is currently at the forefront of cosmology [83]. Light sterile neutrinos or, more generally, a hot dark matter component, can alter the expansion rate at recombination and hence affect the calibration of the standard ruler with which such measurements infer distances. They can, thus, potentially reconcile the discrepancy between these measurements [84–86]. The mass and mixing ranges integral to the simple vacuum oscillation proposals in category **a**), however, are found to be in strong tension [56–58] with those required for this reconciliation. A possible resolution entails the existence of new “secret” interactions between neutrinos [87, 88].
- Sterile neutrinos and/or singlet scalars, which are components of most proposals in categories **a**), **b**) and **c**) both naturally inhabit the dark sector, which may constitute the bulk of matter in the universe. An understanding of the anomalies may then open a portal to the hugely important but unresolved question about the nature of dark matter.

- In general, sterile neutrinos in the mass ranges relevant for category **a)** above impact supernovae neutrino spectra [89, 90] and high energy astrophysical neutrino emission in substantial ways [91–93].
- Almost all proposals that fall in category **b)** above introduce new interactions beyond the SM mediated by a new vector or scalars, resulting in non-trivial consequences for future measurements in collider as well as non-collider experiments. The specifics of each, of course, depend upon the model proposed.
- Many proposals impact other important unresolved issues like the electron [94] and muon $g - 2$ [95–97] anomalies, the origin of neutrino masses, or the KOTO observations [98].

3 The up-scattering interaction, cross section and event rate

Focusing on categories **b)** and **c)**, for our examination, we break up the interaction into two parts. We first consider the tree-level process leading to the up-scattering of an incoming muon neutrino, ν_μ , to a heavy neutral lepton (N_2) in the neutrino detector as shown in figure 1(a), with the underlying assumption that it subsequently decays promptly in the detector. We note that conclusions drawn from this first interaction are applicable to both types of final states, *i.e.* e^+e^- pairs or photons. Final state-specific considerations related to the subsequent decay of the N_2 (figures 1(b) and 1(c)) are examined separately in section 7.

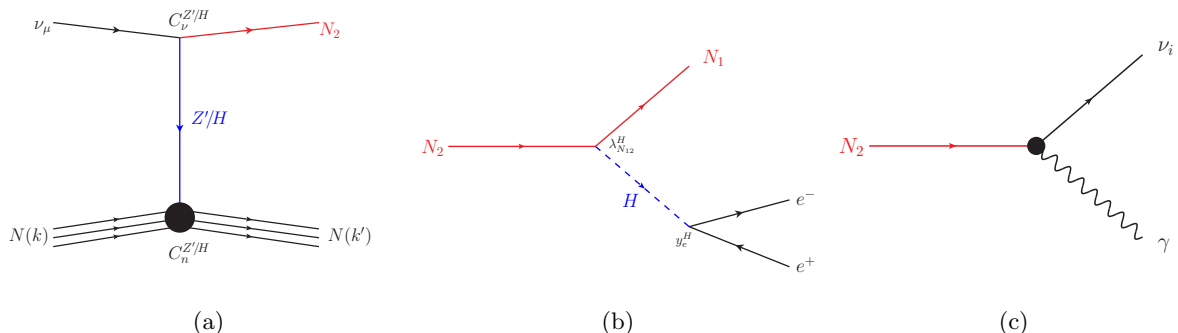


Figure 1. Feynman diagrams for the production and the subsequent decay of the N_2 in LSND and MB.

The mediator for the up-scattering process could be either a light neutral vector boson Z' or a light CP-even scalar H . The relevant interaction Lagrangian for the up-scattering process in each case is given by

$$\mathcal{L}_{\text{int}}^{Z'} = (C_\nu^{Z'} \bar{\nu}_{iL} \gamma^\mu N_{Lj} Z'_\mu + h.c.) + C_n^{Z'} \bar{U}_n \gamma^\mu U_n Z'_\mu, \quad (3.1)$$

$$\mathcal{L}_{\text{int}}^H = (C_\nu^H \bar{\nu}_{iL} N_{Rj} H + h.c.) + C_n^H \bar{U}_n U_n H, \quad (3.2)$$

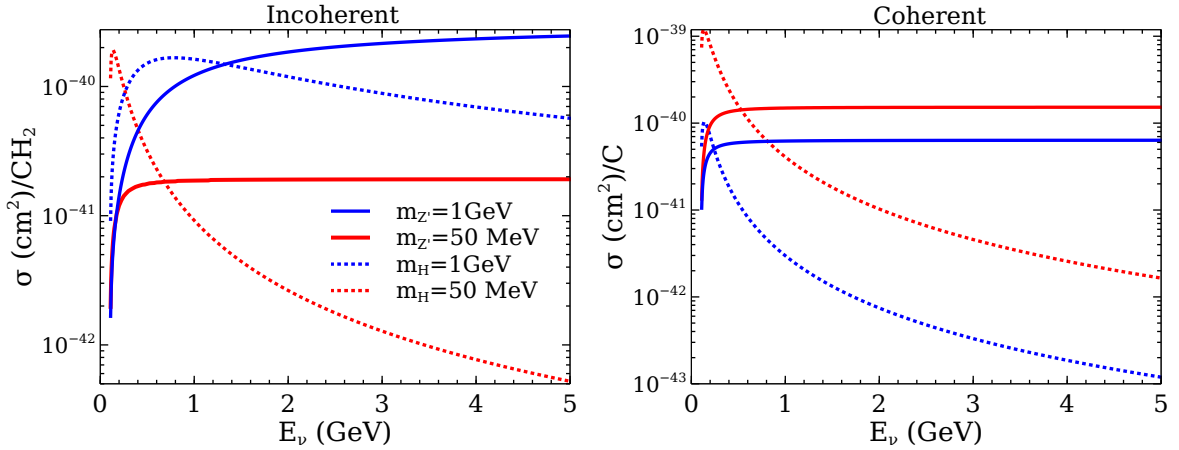


Figure 2. The incoherent (coherent) cross section per CH_2 molecule (C atom) as a function of incoming neutrino energy. The overall constants for different kinds of mediator masses are taken from Table 1.

where U_n is the nucleon field and $i, j = 1, 2, 3$.⁷ For simplicity, we assume that whether the mediator is a Z' or an H , its coupling to a proton is the same as its coupling to a neutron. The up-scattering cross section depends on the overall product of the coupling constants $C_\nu^{Z'} C_n^{Z'}$ ($C_\nu^H C_n^H$) for the vector (scalar) mediator.

The total differential cross section for the production of N_2 mediated by a vector Z' or a scalar H , for the target in MB, *i.e.*, CH_2 , is given by

$$\left[\frac{d\sigma^{Z'/H}}{dE_{N_2}} \right]_{\text{CH}_2} = \left[\underbrace{14(C_\nu^{Z'/H} C_n^{Z'/H})}_{\text{incoherent}} + \underbrace{144(C_\nu^{Z'/H} C_n^{Z'/H})^2 e^{-2b|q^2|}}_{\text{coherent}} \right] \frac{d\sigma^{Z'/H}}{dE_{N_2}}. \quad (3.3)$$

The coherent part of the cross section receives contributions from the entire carbon nucleus (C^{12}), and these decrease as $|q^2| = |(k' - k)^2|$ increases. We implement this by using the form factor $\exp(-2b|q^2|)$ [53], where $b = 25 \text{ GeV}^{-2}$ [53, 102]. The number of N_2 in the final state is given by

$$N_{N_2}^{Z'/H} = \eta \int dE_\nu dE_{N_2} \frac{d\Phi^\nu}{dE_\nu} \left[\frac{d\sigma^{Z'/H}}{dE_{N_2}} \right]_{\text{CH}_2}, \quad (3.4)$$

where Φ^ν is the incoming muon neutrino flux, E_{N_2} and E_ν are the respective energies and η is the signal efficiency of the detector.

A substantial amount of information about the viability of various solutions can be gleaned from focussing simply on the production of N_2 in the final state. To calculate

⁷We have assumed the presence of three right-handed neutrinos, as is usual for generating neutrino mass, although our interaction only requires two such particles (N_1 and N_2). Additionally, these neutrinos are assumed to be Majorana in nature, which is relevant when we consider the decay of N_2 in what follows. We note that angular distributions for the decay of Majorana neutrinos differ from those for Dirac neutrinos. Specifically, in the Majorana case, the angular distribution of the daughters in the decay of a heavy neutrino into a lighter neutrino and a self-conjugate boson is isotropic in the parent's rest frame [99–101], a fact that we use in our considerations.

Mediator Mass	$C_\nu^{Z'} C_n^{Z'}$	$C_\nu^H C_n^H$
50 MeV	1.04×10^{-8}	9.3×10^{-8}
1 GeV	8.5×10^{-7}	2.14×10^{-6}
300 MeV	–	5.35×10^{-7}

Table 1. The values of the overall couplings for the vector and scalar mediators for different values of mediator masses to produce 560 N_2 in the MB final state. The mass of N_2 is 100 MeV.

the total number of N_2 , we use the signal efficiencies of the LSND and MB experiments provided in [4, 5] and references therein. The actual signal in the detector depends on the mechanism of the decay of N_2 to a γ or an e^+e^- pair. However, for our purpose in this section, we assume that the signal arises from N_2 decay in the detector, and adjust the values of the couplings so as to produce a total of 560 N_2 in the final state. This number corresponds to the central value of the excess observed [4] over the SM expectation during the neutrino run, given the total exposure so far, and represents, in some sense, the minimum number of N_2 that should be produced. The events are calculated using eqs. (3.3),(3.4) and the assumed values of the product of couplings are provided in Table 1.

Finally, it is appropriate to comment on the role that nuclear effects may play in scenarios of new physics that involve incoherent scattering, like the ones considered here. For known neutrino-nuclear cross sections, several techniques are in use [103–108]. At lower energies (*e.g.* at LSND) shell-model techniques yield good results. At somewhat higher, *i.e.* intermediate energies (several hundred MeVs to a few GeV) the Continuum Random Phase Approximation (CRPA) has been successfully used to show that nuclear effects are relevant mostly at low momentum transfers, while at higher energies the Fermi gas model has worked well. Overall, these techniques have been used in conjunction with experimental data in order to obtain a better understanding of these interactions. Additionally, for energies up to ~ 1 GeV, the role of final state interactions may be relevant [109, 110]. While it is reasonable to assume, as we do here, that similar considerations will apply in the case of new physics scenarios, only further studies can confirm the validity of such an assumption. We do not undertake them here, as they would be outside the scope of this paper⁸.

4 Requirements resulting from the variation of the cross section with incoming neutrino energy and with mediator mass

The variation of the up-scattering cross section with incoming neutrino energy depends on the type of mediator, as shown in figure 2. The left panel shows the incoherent cross section while the right panel corresponds to the coherent cross section for vector (Z' , solid curves) and scalar (H , dotted curves) mediators for two values of the mediator mass, (50 MeV (red) and 1 GeV (blue)) for a CH_2 target.

We see that the scalar and vector mediated cross sections behave distinctly, and our representative calculations bring out the following qualitative points:

⁸We have, nonetheless, put in a cut of a minimal requirement of 8 MeV for a neutron to exit the nucleus.

- While in all cases the cross section initially rises as the energy is increased from its lowest values, it subsequently drops for a scalar mediator whereas it remains approximately flat with increasing energy for a vector mediator. Both the coherent and incoherent parts exhibit this general behaviour. It is this relatively rapid drop in the cross section for H as the neutrino energy rises that allows solutions with a scalar mediator to comfortably avoid constraints coming from CHARM II [111] and MINER ν A [112], compared to the Z' mediated process. We recall that the $\nu - e$ scattering measurements in both these experiments can in principle put tight constraints [74] on the model that explains the LEE. The coherent signal seen by them, ($\nu_\mu + A \rightarrow N_2 + A \rightarrow N_1 + e^+ + e^- + A$) could mimic a charged or neutral current $\nu - e$ event. Hence, a large coherent contribution, as is present in the Z' case, will be in conflict with the $\nu - e$ scattering measurements of CHARM II and MINER ν A.
- We also note from figure 2 that the coherent contribution dominates over the incoherent part for lighter mediator masses, whereas the opposite is true for the higher mass choice for both types of mediators. Thus lighter mediators tend to make large coherent contributions, and since these tend to be forward in angle, they help populate event bins for $\cos\theta \simeq 1$, a point that we explore further in section 5.
- We note that for LSND, contributions to events stem from the incoherent part of the cross section only, given the presence of a neutron in the final state. We thus focus on the region in the left panel of figure 2, and note the behaviour as the energy drops from MB (~ 800 MeV) to LSND DAR flux values ($\sim 150 - 200$ MeV). We see that for the higher mass mediators ($m_{Z'/H} = 1$ GeV; blue curves), while the incoherent cross section drops for both mediators, the vector cross section has lower values to begin with compared to the scalar and also drops rapidly. For instance, it can be seen that the cross section for the Z' drops an order of magnitude over this energy range for $m_{Z'} = 1$ GeV.

For the lighter mass choices ($m_{Z'/H} = 50$ MeV; red curves), the incoherent scalar cross section is significantly higher than the vector one over this energy range, and in fact increases as the energy is lowered, unlike its vector counterpart. This reduction in the incoherent vector cross section at values below MB energies (< 800 MeV) makes it more difficult for models with an additional vector mediator to give a sufficient number of electron-like excess events at LSND, even though a high enough Z' mass may allow one to successfully evade the CHARM II and MINER ν A bounds. On the other hand, too low a scalar mediator mass results in many more events than those observed in LSND, both in the 20 – 60 MeV visible energy range which recorded data, and beyond 60 MeV, where only a limited number of events were seen.

- Finally, we point out an important constraint that applies to models which use scalar mediators, especially those with low masses $m_H \simeq 100$ MeV. As can be seen in figure 2 the cross section tends to rise at low values of the incoming neutrino energy. However, in such models, if N_2 decays primarily invisibly, as in [21], the incoherent

interaction would mimic the neutral current interaction $\nu N \rightarrow \nu N$, which has been measured at MB [113] at these energies, and found to be in agreement with the SM. Conformity with this measurement is thus an important restriction on such models.

Overall, the cross section and mediator mass considerations for a common solution thus appear to favour scalar mediators over vectors. Secondly, our representative calculations also point to a preference for lighter (but not ultra-light) mediators if both excesses are to have a simultaneous solution.

We next provide some example numbers to quantitatively illustrate these qualitative conclusions:

Assuming a mediator mass of 1 GeV, we fit the MB events by considering the appropriate values of $C_\nu^{Z'} C_n^{Z'}$ and $C_\nu^H C_n^H$. Now using the same coupling values, we calculate the number of produced N_2 of mass 100 MeV in LSND. We find that:

- To produce 560 N_2 in final state of MB, the required value of $C_\nu^{Z'} C_n^{Z'}$ is 8.5×10^{-7} . These couplings, yield around 7 N_2 in LSND instead of the required number of 32 [5].
- For the scalar mediator, the necessary value of $C_\nu^H C_n^H$ is 2.14×10^{-6} , obtained from the MB fit. Using the same coupling constant, we get around 35 events in LSND.

We see in this example that while both mediators fit MB total events, the scalar mediator produces 5 times more events compared to the Z' in LSND.

Additionally, as mentioned above, the different behaviour exhibited by the vector also places more restrictions on it constraint-wise than it does on the scalar. Noting, from the right panel of figure 2, that the coherent contribution to the cross section increases as the mediator mass decreases, we find that the mass of Z' should be approximately 500 MeV to avoid the CHARM II and MINER ν A constraints discussed above, if it has to concurrently produce 560 N_2 in MB. On the other hand, no such restriction results for the scalar, since the coherent cross section drops rapidly as it approaches CHARM II ($\langle E_\nu \rangle = 24$ GeV, $\langle E_{\bar{\nu}} \rangle = 19$ GeV) and MINER ν A ($\langle E_\nu \rangle = 6$ GeV) energies.

5 Requirements resulting from fitting the angular distribution in MB

An examination of the angular distribution of MB is also useful from the point of view of imposing requirements on proposed solutions. The excess in MB is distributed over all directions, but is moderately forward. Figure 3 shows, bin-wise, the cross section responsible for the production of N_2 as a function of the cosine of the angle between the momentum direction of N_2 and the beam direction⁹. The incoming neutrino energy is fixed at 800 MeV and $m_{N_2} = 100$ MeV for all panels. Both the coherent (red) and incoherent (green) contributions are shown. From the upper and lower left panels, we see that when the mass of the mediator is low, (50 MeV), almost all the produced N_2 are in the first (*i.e.*

⁹We have checked that this is a good approximate indicator of the eventual angle that the signal will form with the beam, once N_2 decays.

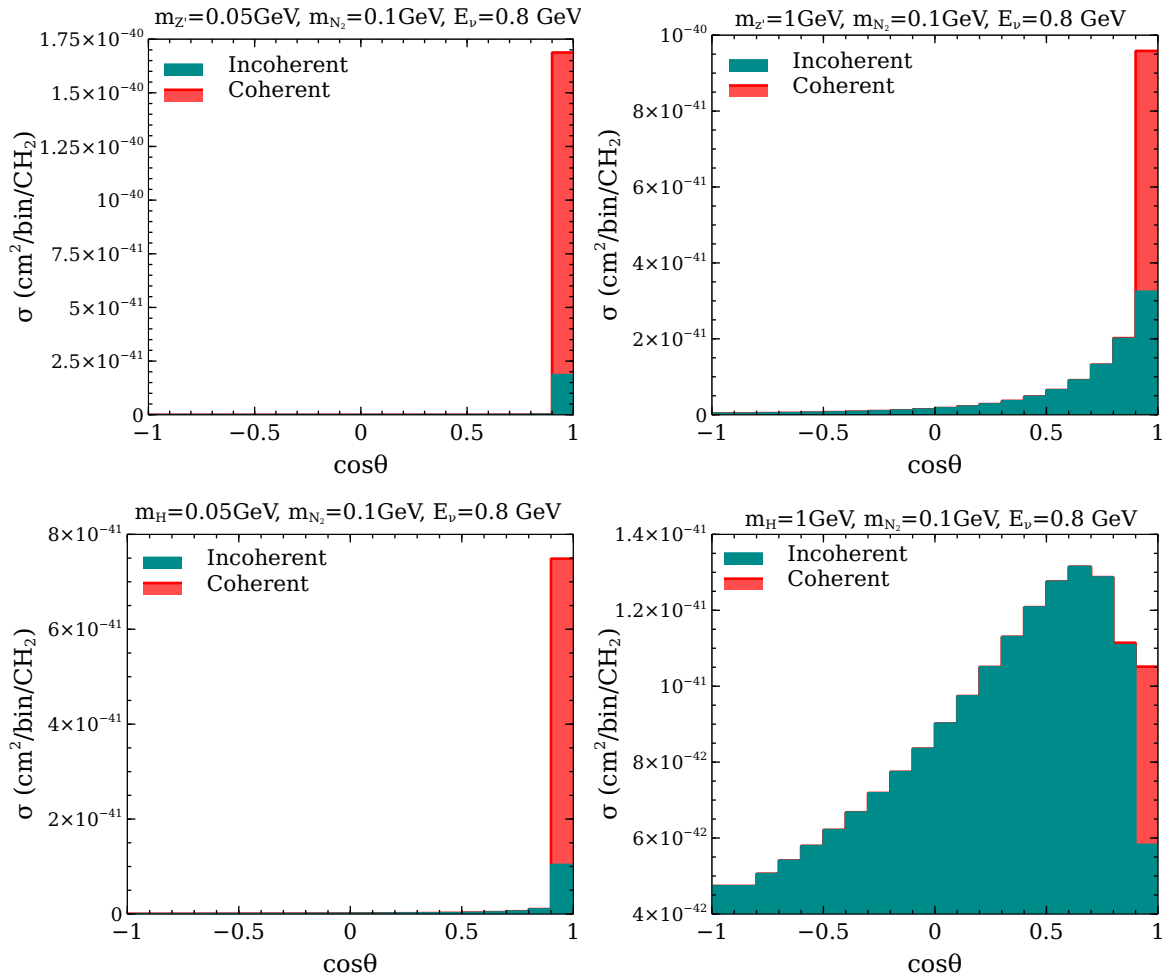


Figure 3. Angular variation of the total cross section for two different mass choices of light scalar and light vector mediators. Both coherent and incoherent contributions are shown.

most forward) bin for both a scalar and a vector mediators. As the mass of the mediator is increased to 1 GeV (right panels), the distribution shifts and the other bins are also populated for both types of mediators, although the shifts are qualitatively different.

One way to counter balance the effect of a low mass mediator on the angular distribution is to increase the mass of N_2 . The energy budget set by the incoming muon neutrino ($E_\nu \sim 1$ GeV) then reduces the kinetic energy of the N_2 and drives the distribution towards greater isotropy once it decays to *e.g.* an e^+e^- pair. An example of this is provided by the proposed solution to MB in [18], where the benchmark point assumes a vector mediator mass of ~ 30 MeV and an N_2 mass of ~ 420 MeV to get the required angular distribution. A common solution to both the LSND and the MB anomalies, however, is disallowed by such a choice, since the neutrino energies at LSND are much smaller, with no flux beyond $E_\nu \sim 250$ MeV. Thus, while a heavier mediator or a heavier N_2 both assist in getting the desired MB angular distribution, a common solution that also helps us understand LSND

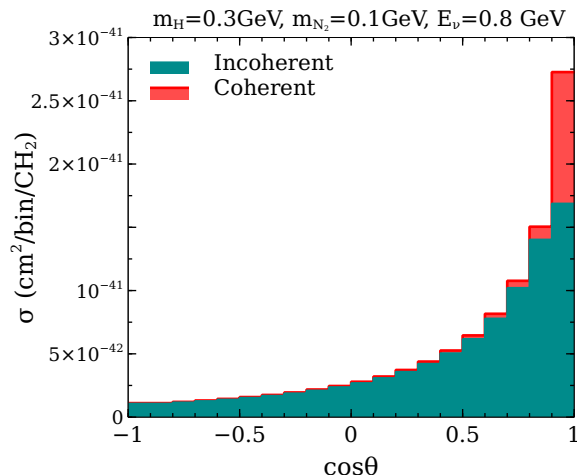


Figure 4. Angular variation of the total cross section with an intermediate mass scalar. Both coherent and incoherent contributions are shown.

suggests the use of an N_2 mass closer to 100 MeV, while using a heavier mediator with a mass ~ 1 GeV. Using these trial values in the right panels of figure 3, however, shows that a vector mediator over-produces the forward events (*i.e.* those in the first bin), whereas the scalar mediator under-produces them.

From the previous section which considers the effects of mediator mass and energy on the cross section keeping constraints in mind, we found that these criteria point to the scalar mediator as being preferred over the vector. The considerations in this section suggest, among other things, that using a single scalar mediator and adjusting its mass as well as the mass of N_2 will allow us to find both a common solution to the two anomalies as well as match the angular distribution in MB. While an N_2 mass of 100 MeV is a good ball-park value, one must also keep in mind that as this is lowered, the event rate at LSND rises quickly beyond what was observed. A sample choice that has the potential to achieve an appropriate balance is shown in figure 4, along with the chosen parameter values; in particular, the scalar mass used is 300 MeV.

Our generic arguments so far have led us to the conclusion that one can achieve a fit to both LSND and MB data using a heavy neutrino of about ~ 100 MeV which decays to give the visible signal from an interaction that is mediated by a scalar of mass ~ 300 MeV. In general, such a solution usually requires the addition of a singlet scalar that mixes with the SM Higgs boson to generate interactions with quarks and leptons. Constraints on such models arise from a variety of different experiments, and are unusually tight, often forcing the mixing to be very low and making it difficult to explain significant excesses above SM backgrounds without further additions to the particle spectrum, as, *e.g.* in [28]. Some of the important constraints are from NA62 [114], E949 [115], CHARM [116], NA48/2 [117], LHCb [118, 119] and Belle [120].

Finally, we remark that we have examined the fit to the LSND angular distribution for

the 300 MeV scalar considered above. We find that acceptable fits may be possible, but given the uncertainty and limited range of the measured LSND distributions, it is difficult to draw any firm conclusions based on this, especially as we consider the N_2 distributions as an approximation to the actual distribution of the final state.

6 Requirements resulting from considerations related to the energy distributions in LSND and MB

Proceeding on the basis of what we have learnt with respect to requirements in the previous sections, we next examine if the observed energy distributions in LSND and MB can provide additional information. In principle, one has the freedom to choose the masses of the mediator, N_1 and N_2 . Recalling that $m_{N_2} \sim 100$ MeV and a single 300 MeV scalar mediator appear to be reasonable choices in our search for acceptable benchmarks and putting the constraint considerations mentioned above which restrict a 300 MeV singlet scalar aside for the moment, we examine its effect on the energy distributions. As above, we assume that N_2 once produced, decays to a second lighter heavy sterile neutrino N_1 (or ν_i) and either a γ or an e^+e^- pair. Figure 5 shows the distributions for MB and LSND for three different choices of the N_1 mass (60 MeV, 100 MeV, 140 MeV), two different mass values of N_2 (135 MeV in the first two rows and 180 MeV in the bottom row) and a fixed mass value of 300 MeV for the scalar mediator. We note that the scalar mediates both the interaction that produces N_2 and the subsequent decay leading to the signal.

Considered in conjunction, the panels in figure 5 reflect the difficulties in obtaining a good fit simultaneously for the MB and LSND energy distributions if a single scalar is used. The top panels, where a relatively low mass of N_2 is assumed, provides a reasonable fit to the MB distribution. On the other hand, while not apparent in the figure, the low mass pushes the LSND distribution to the right, leading to too many events with energies greater than 60 MeV, which were not seen. On increasing the N_2 mass moderately, to 100 MeV (middle panels) one finds that while the LSND distribution appears to have a shape closer to that which was observed, the total number of events is much higher than required. The MB fit worsens compared to the top panel, with events being underproduced. It is possible to reduce the total number of events in LSND by increasing the mass of N_2 , which is what we attempt to do in the bottom panels. This certainly improves the LSND fit, but the MB distribution, although shifted, continues to significantly underproduce events in many bins, especially in the 250 MeV to 550 MeV range. In general, attempts to fit LSND will cause a depletion in the low and/or medium energy bins of MB, which contain the bulk of its event excess. For example, the total number of MB events in the bottom left panel is 294 compared to the observed value of 560. We also note the reason for the overproduction of events in many cases in LSND: this is because cuts which ensure that the pairs produced in MB mimic the signal of a single charged lepton have been applied. These consist in requiring a) that the opening angle between the pair is $\leq 10^\circ$ or, b) in the case of an asymmetric pair, the softer partner carries an energy ≤ 30 MeV. Once this is done, only about 20–30% of total MB events survive. This requires us to have a higher coupling when fitting MB, which, when used to calculate the LSND events, where no cuts are applied,

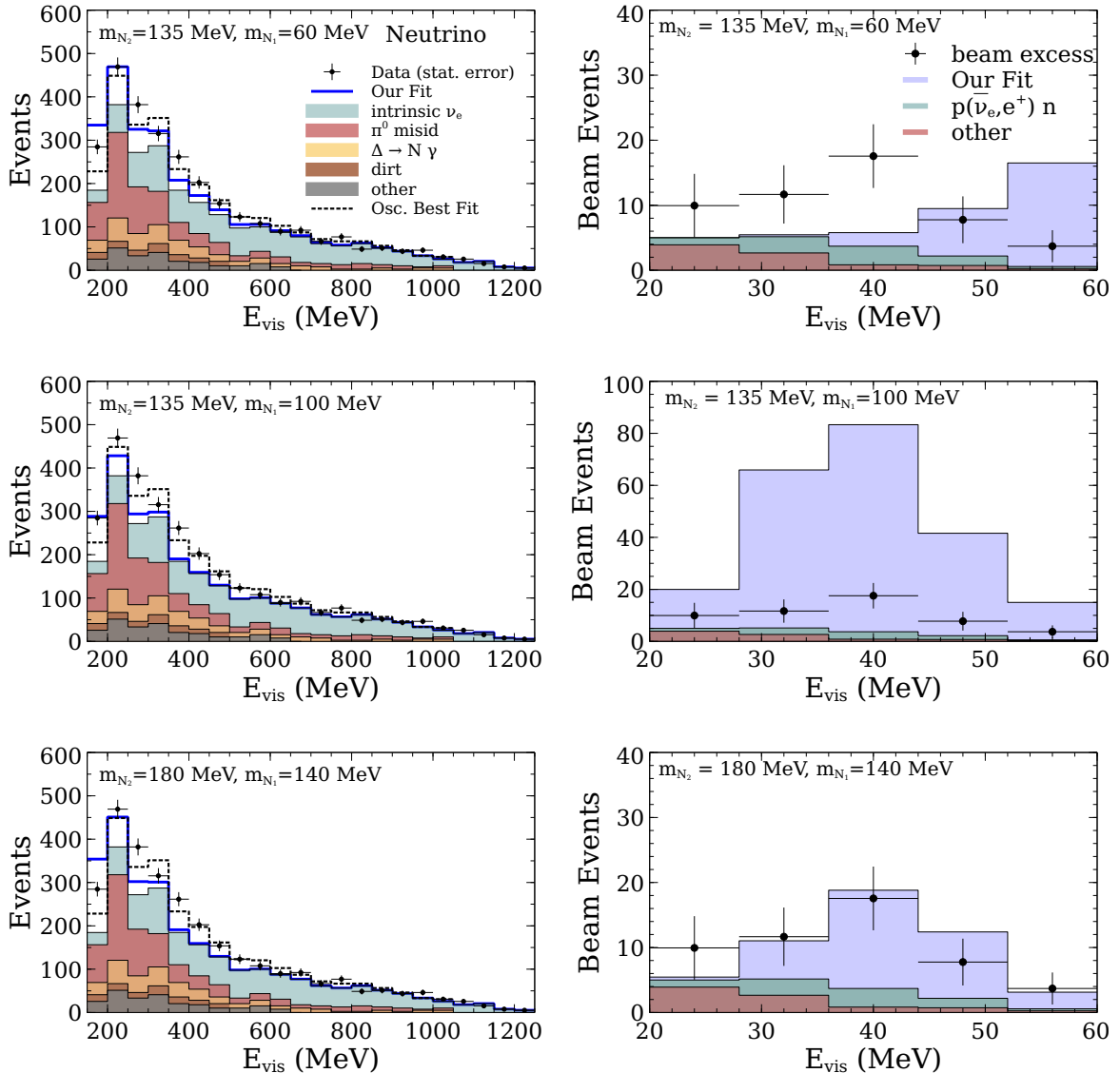


Figure 5. The left (right) column corresponds to the MB (LSND) events as a function of the visible energy, E_{vis} . Various values of the masses of the daughter particle, m_{N_1} are shown in the plot. The mass of the single scalar is fixed at 300 MeV for all panels while the mass of the decaying particle N_2 is assumed to be 135 MeV for the top and middle panels and 180 MeV in the bottom panel.

leads to a corresponding higher number¹⁰. This behaviour is aided by the tendency of the incoherent scalar mediated cross section to rise as the energy is lowered from MB to LSND values, as clearly seen from figure 2 (left panel).

¹⁰The same behaviour is expected in the case of a vector mediator. However, as we have discussed earlier, vector mediators are subject to strong cross section constraints.

7 Requirements resulting from considerations related to the visible signal in LSND and MB

A detailed study of the requirements stemming from the observed signal (figures 1(b) and 1(c)) depends on specifics of the model employed, which is beyond the scope of this work. Hence in this section we restrict ourselves to certain general observations as well as point to constraints which must be kept in mind.

The simplest possibilities which could mimic an electron-like signal in new physics scenarios are either a γ or a collimated e^+e^- pair, which, in the scenario considered here, result from the decay of N_2 , generically governed by one of the following interaction Lagrangians:

$$\mathcal{L}_{\text{int}} \supset \lambda_{N_{12}}^H \bar{N}_1 N_2 H + y_e^H \bar{e} e H, \quad (7.1)$$

$$\mathcal{L}_{\text{int}} \supset \mu_{\text{tr}} \bar{\nu}_{iL} \sigma_{\mu\nu} F^{\mu\nu} N_{R2}, \quad (7.2)$$

where $\lambda_{N_{12}}^H$ and y_e^H are Yukawa couplings. μ_{tr} is the neutrino transition magnetic moment, $F^{\mu\nu}$ is the electromagnetic field strength tensor and $\sigma_{\mu\nu} = \frac{i}{2}[\gamma_\mu, \gamma_\nu]$.

From kinematics, N_2 (~ 150 MeV) cannot decay to an on-shell scalar of mass ~ 300 MeV, which are the preferred ball-park mass values we have identified for the heavy sterile neutrino and the mediator respectively from the discussions in previous sections. The decay process could happen via the off-shell exchange of the scalar, with $N_2 \rightarrow N_1 + e^+ + e^-$. A discussion of constraints related to the production of an e^+e^- pair in the final state is provided in [24, 64, 72–74].

In general, the kinematics of three-body decay allows the pair to have an energy greater than $\frac{1}{2}m_{N_2}$ in the rest frame of N_2 (unlike two-body decay). This is all the more possible if N_1 is relatively light, *i.e.* $m_{N_1} \leq 60$ MeV, or if one were to consider the signal as arising from $N_2 \rightarrow \nu_i + e^+ + e^-$, where ν_i is an active SM neutrino. Overall, because of this, the three-body decay option which one is forced into when the mediator mass exceeds that of N_2 thus tends to give too many excess events in LSND beyond visible energies of 60 MeV, in conflict with observations. This last consideration also holds for the case where the excess results from $N_2 \rightarrow \nu_i + \gamma$, mediated by a transition magnetic moment¹¹. Depending on the model details, solutions where the signal arises due to a photon coupling via a magnetic moment must contend with strong constraints on either active-sterile mixing and/or magnetic moments [55, 66–70, 75, 77–80] or from the requirement to match the observed angular distribution in MB [81].

An additional important restriction for the three-body decay situation arises from mono-photon searches at BaBar [121]. These put a tight constraint on a dark photon (A') that decays invisibly. The bound on the kinetic mixing parameter ε is $(e\varepsilon)^2 < 9 \times 10^{-8}$ for $m_{A'} \lesssim 6$ GeV coming from the process $e^+e^- \rightarrow \gamma A'$; $A' \rightarrow$ invisibles, where $e \simeq 0.3$ is the electric charge. This strong limit on ε can be relaxed if the A' decays semi-visibly inside the detector *i.e.* $\text{BR}(A' \rightarrow \text{visible particle} + \text{missing energy}) \simeq 1$ [122, 123]. For our purpose here, the light scalar (H) will be produced along with a γ in e^+e^- collision.

¹¹The process $N_2 \rightarrow N_1 + \gamma$ is also possible. In the simplest case this would proceed via mixing with SM neutrinos but would be highly suppressed. Other possibilities would be model dependent, for example, via a charged Higgs in the model discussed in [24].

Since H also decays semi-visibly via $H \rightarrow N_1 + N_2 \rightarrow N_1 + N_1 + e^+ + e^-$ with almost 100% branching ratio, the resultant constraint on y_e^H can be relaxed so that N_2 decays promptly within the LSND and MB detectors. Similar considerations were used in Ref. [23]. Our calculations here use an effective coupling ($y_e^H \lambda_{N_{12}}^H$) of 9×10^{-4} to enable this, which gives a decay length of $\mathcal{O}(\sim \text{few cm})$ for N_2 .

8 Discussion

Our examination of the cross section behaviour with energy and its dependence on the mediator mass (section 3) suggests that a common solution is simpler to achieve using scalar mediators as opposed to vectors. Vector solutions which are likely to provide reasonable fits to the angular and energy distributions in MB tend to give lower cross sections than required when it comes to LSND, producing too few events once the new physics parameters are fixed by a MB fit. Such mediators also have cross sections which stay flat in this energy range as the neutrino energy increases, which makes it difficult to satisfy constraints from higher energy experiments like CHARM II [111], MINER ν A [112] and IceCube [71, 76].

Two additional considerations which apply to vector solutions are:

- In their search for a final state photon produced by Δ production and decay [11], MicroBooNE found no evidence of an excess. In models with an additional vector which can mediate the interaction, an additional contribution to Δ production is expected to occur, rendering them potentially in tension with this observation if this contribution is statistically significant.
- Any new light vector with dimension-4 couplings to the SM fermions must couple to a conserved current. If this is not the case, processes with $(\text{energy}/\text{vector mass})^2$ rates involving the longitudinal mode of the new vector can be the dominant production mechanism in high-energy experiments, which places strong constraints on its coupling [124–126].

Considerations based on the observed angular distributions in LSND and MB are discussed in section 5. The experimentally observed distribution for MB is fairly forward, but the excess extends in all directions, although it becomes smaller as we move away from the $\cos \theta \simeq 1$ values. As expected, lighter mediators, whether scalar or vector, favour low momentum transfers to the target and hence tend to populate the forward direction more so than heavier ones. As the mediator mass is increased, other angular bins get populated, while the forward direction, which is dominantly populated in the observed distribution, gets depleted. We find that an intermediate mass mediator does offer the possibility of a reasonable fit to the observed angular features in MB. However, considerations based on the observed energy distributions in the two experiments, which we have examined in section 6 above, disfavour a single intermediate mass scalar mediator, because it becomes difficult to simultaneously find good fits to the observed energy distributions in LSND and MB.

Thus, overall, energy distributions in LSND and MB, the angular distribution in MB, when combined with the stringent constraints on light singlet scalars, suggest the use of a

scalar doublet, with one light and one moderately heavy partner. This allows for a degree of angular isotropy as well as a large number of events in the forward direction, as were observed. With respect to energy distributions, the lighter partner tends to help give the correct distribution in LSND, while heavier partners tend to distort it. As one moves from MB energies down to LSND energies, the incoherent cross section (relevant for LSND) for heavier mediators drops much more rapidly than lighter mediators, which consequently contribute more to the total events. Thus, a combination of a moderately heavy and a light mediator complement each other well when a common solution to the two anomalies is sought. An example solution to both anomalies that incorporates all the features that have emerged in our study has been provided in [24].

Our approach has been phenomenological, keeping simplicity and minimality as guiding principles to the extent possible. Our results should be treated as indicative, and not definitive, since it will always be possible to construct models that circumvent specific obstacles. Such efforts would, however, extract a price in terms of increased complexity in the number of particles and new interactions invoked. We stress that the requirements we obtain above pertain to *simultaneous* solutions which attempt to explain both the LSND and MB anomalies, and can be considerably different if this condition is relaxed.

9 Conclusions

In this work, we have focussed on an important class of common, non-oscillation new physics solutions to the LSND and MB excesses, keeping the recent MicroBooNE results in mind. It comprises of solutions which have an e^+e^- pair or a photon produced inside the detector via a new interaction involving the up-scattering of a heavy sterile neutrino and its subsequent decay. We have used cross section magnitudes and variation with energy and angle as well as existing constraints to arrive at conclusions which point to scalar mediators being favoured over vectors, and to one light ($\lesssim 50$ MeV) and one moderately heavy ($\lesssim 850$ MeV) mass mediator being a better choice than a single scalar of intermediate mass.

The insistence on a solution that resolves both excesses simultaneously is, of course, a choice. It restricts and guides potential solutions in ways that attempts to address the anomalies individually do not. It is, however, remarkable that once this is demanded, and the dictates of the cross section, the observed energy and angular distributions in both experiments as well as the many constraints from various experiments adhered to (this work), then one is led to a simple extension of the SM that i) resolves both anomalies, ii) provides a portal to the dark sector, iii) accounts for the experimentally observed value of the muon $g - 2$ and iv) addresses the issue of neutrino mass via a Type I seesaw, in conformity with the observed values of neutrino mass-squared differences in oscillation experiments, as shown in [24].

Additionally, we have made an effort to emphasise that understanding the LSND and MB results in conjunction with MicroBooNE provides both a high-stakes challenge as well as an unprecedented opportunity for the discovery of physics beyond the SM. An oft-repeated statement in the literature is that the only physics discovery beyond the SM,

since its inception over fifty years ago is that neutrinos are massive. While the theoretical, phenomenological and experimental consequences of neutrino mass have been profound, altering our approach to and understanding of neutrino physics, cosmology, stellar evolution, dark matter, leptogenesis and CP violation, it is also true that the *structural* change in the SM necessary to accommodate it is relatively benign, requiring the addition of right-handed neutrinos only¹². If indeed, the present results that are the subject of this paper do herald new physics, this is likely *not* to be the case. All of the proposals for the three possible final states (single electrons, an e^+e^- pair or a photon) require non-trivial new physics. In particular, those giving an e^+e^- pair do not have a known SM background, and appear to call for new particles and interactions, as well as some portal to the dark sector, indicating possibly major additions to the particle spectrum and the interactions between them.

It is fortuitous that all three types of possible final states will be tested soon, first in MicroBooNE and then in the other detectors comprising the Fermilab short baseline program.

The anticipation is palpable.

Acknowledgments

RG is grateful to William Louis for his help with our many questions on LSND, MB and MicroBooNE. He would also like to express appreciation of the many interesting conversations he has had with Boris Kayser and GERALYN Zeller on the anomalies which are the subject of this paper.

WA, RG and SR also acknowledge support from the XII Plan Neutrino Project of the Department of Atomic Energy and the High Performance Cluster Facility at HRI (<http://www.hri.res.in/cluster/>).

References

- [1] C. Athanassopoulos et al. (LSND), Phys. Rev. C **54**, 2685 (1996), [nucl-ex/9605001](#).
- [2] A. A. Aguilar-Arevalo et al. (MiniBooNE), Phys. Rev. Lett. **102**, 101802 (2009), [0812.2243](#).
- [3] A. A. Aguilar-Arevalo et al. (MiniBooNE), Phys. Rev. Lett. **121**, 221801 (2018), [1805.12028](#).
- [4] A. A. Aguilar-Arevalo et al. (MiniBooNE), Phys. Rev. D **103**, 052002 (2021), [2006.16883](#).
- [5] A. Aguilar-Arevalo et al. (LSND), Phys. Rev. D **64**, 112007 (2001), [hep-ex/0104049](#).
- [6] C. Athanassopoulos et al. (LSND), Nucl. Instrum. Meth. A **388**, 149 (1997), [nucl-ex/9605002](#).
- [7] T. Katori (MiniBooNE), in *3rd World Summit on Exploring the Dark Side of the Universe* (2020), pp. 139–148, [2010.06015](#).

¹²This is true irrespective of whether they are Majorana or Dirac particles, albeit the mass scales at which these neutrinos enter the theory can be very different for the two.

- [8] B. Dasgupta and J. Kopp, Phys. Rept. **928**, 63 (2021), [2106.05913](#).
- [9] V. Brdar and J. Kopp (2021), [2109.08157](#).
- [10] L. Alvarez-Ruso and E. Saul-Sala (2021), [2111.02504](#).
- [11] P. Abratenko et al. (MicroBooNE) (2021), [2110.00409](#).
- [12] R. Acciarri et al. (MicroBooNE), JINST **12**, P02017 (2017), [1612.05824](#).
- [13] P. Abratenko et al. (MicroBooNE) (2021), [2110.13978](#).
- [14] P. Abratenko et al. (MicroBooNE) (2021), [2110.14054](#).
- [15] P. Abratenko et al. (MicroBooNE) (2021), [2110.14065](#).
- [16] P. Abratenko et al. (MicroBooNE) (2021), [2110.14080](#).
- [17] A. A. Aguilar-Arevalo et al. (MiniBooNE), Phys. Rev. **D81**, 013005 (2010), [0911.2063](#).
- [18] E. Bertuzzo, S. Jana, P. A. N. Machado, and R. Zukanovich Funchal, Phys. Rev. Lett. **121**, 241801 (2018), [1807.09877](#).
- [19] P. Ballett, S. Pascoli, and M. Ross-Lonergan, Phys. Rev. D **99**, 071701 (2019), [1808.02915](#).
- [20] P. Ballett, M. Hostert, and S. Pascoli, Phys. Rev. D **101**, 115025 (2020), [1903.07589](#).
- [21] B. Dutta, S. Ghosh, and T. Li, Phys. Rev. D **102**, 055017 (2020), [2006.01319](#).
- [22] W. Abdallah, R. Gandhi, and S. Roy, JHEP **12**, 188 (2020), [2006.01948](#).
- [23] A. Abdullahi, M. Hostert, and S. Pascoli (2020), [2007.11813](#).
- [24] W. Abdallah, R. Gandhi, and S. Roy, Phys. Rev. D **104**, 055028 (2021), [2010.06159](#).
- [25] S. N. Gninenko, Phys. Rev. Lett. **103**, 241802 (2009), [0902.3802](#).
- [26] S. N. Gninenko, Phys. Rev. D **83**, 015015 (2011), [1009.5536](#).
- [27] O. Fischer, A. Hernández-Cabezudo, and T. Schwetz, Phys. Rev. D **101**, 075045 (2020), [1909.09561](#).
- [28] A. Datta, S. Kamali, and D. Marfatia, Phys. Lett. B **807**, 135579 (2020), [2005.08920](#).
- [29] B. Dutta, D. Kim, A. Thompson, R. T. Thornton, and R. G. Van de Water (2021), [2110.11944](#).
- [30] S. Vergani, N. W. Kamp, A. Diaz, C. A. Argüelles, J. M. Conrad, M. H. Shaevitz, and M. A. Uchida, Phys. Rev. D **104**, 095005 (2021), [2105.06470](#).
- [31] G. Mention, M. Fechner, T. Lasserre, T. A. Mueller, D. Lhuillier, M. Cribier, and A. Letourneau, Phys. Rev. D **83**, 073006 (2011), [1101.2755](#).
- [32] C. Giunti and M. Laveder, Phys. Rev. C **83**, 065504 (2011), [1006.3244](#).
- [33] V. V. Barinov et al. (2021), [2109.11482](#).
- [34] S. Gariazzo, in *17th International Conference on Topics in Astroparticle and Underground Physics* (2021), [2110.09876](#).
- [35] S. Schoppmann, Universe **7**, 360 (2021), [2109.13541](#).
- [36] C. A. Argüelles et al., Rept. Prog. Phys. **83**, 124201 (2020), [1907.08311](#).
- [37] A. Diaz, C. A. Argüelles, G. H. Collin, J. M. Conrad, and M. H. Shaevitz, Phys. Rept. **884**, 1 (2020), [1906.00045](#).

- [38] P. A. Machado, O. Palamara, and D. W. Schmitz, *Ann. Rev. Nucl. Part. Sci.* **69**, 363 (2019), [1903.04608](#).
- [39] D. S. M. Alves, W. C. Louis, and P. G. deNiverville (2022), [2201.00876](#).
- [40] J. Asaadi, E. Church, R. Guenette, B. J. P. Jones, and A. M. Szec, *Phys. Rev.* **D97**, 075021 (2018), [1712.08019](#).
- [41] S. Palomares-Ruiz, S. Pascoli, and T. Schwetz, *JHEP* **09**, 048 (2005), [hep-ph/0505216](#).
- [42] Y. Bai, R. Lu, S. Lu, J. Salvado, and B. A. Stefanek, *Phys. Rev. D* **93**, 073004 (2016), [1512.05357](#).
- [43] Z. Moss, M. H. Moulai, C. A. Argüelles, and J. M. Conrad, *Phys. Rev. D* **97**, 055017 (2018), [1711.05921](#).
- [44] M. Dentler, I. Esteban, J. Kopp, and P. Machado, *Phys. Rev. D* **101**, 115013 (2020), [1911.01427](#).
- [45] A. de Gouvêa, O. L. G. Peres, S. Prakash, and G. V. Stenico, *JHEP* **07**, 141 (2020), [1911.01447](#).
- [46] P. B. Denton (2021), [2111.05793](#).
- [47] C. A. Argüelles, I. Esteban, M. Hostert, K. J. Kelly, J. Kopp, P. A. N. Machado, I. Martinez-Soler, and Y. F. Perez-Gonzalez (2021), [2111.10359](#).
- [48] A. A. Aguilar-Arevalo et al. (MiniBooNE) (2022), [2201.01724](#).
- [49] T. A. Mueller et al., *Phys. Rev. C* **83**, 054615 (2011), [1101.2663](#).
- [50] P. Huber, *Phys. Rev. C* **84**, 024617 (2011), [Erratum: *Phys.Rev.C* 85, 029901 (2012)], [1106.0687](#).
- [51] C. Giunti, Y. F. Li, C. A. Ternes, and Z. Xin (2021), [2110.06820](#).
- [52] C.-H. V. Chang, C.-R. Chen, S.-Y. Ho, and S.-Y. Tseng, *Phys. Rev. D* **104**, 015030 (2021), [2102.05012](#).
- [53] R. J. Hill, *Phys. Rev.* **D81**, 013008 (2010), [0905.0291](#).
- [54] E. Wang, L. Alvarez-Ruso, and J. Nieves, *Phys. Rev. C* **89**, 015503 (2014), [1311.2151](#).
- [55] G. Magill, R. Plestid, M. Pospelov, and Y.-D. Tsai, *Phys. Rev. D* **98**, 115015 (2018), [1803.03262](#).
- [56] J. M. Berryman, *Phys. Rev. D* **100**, 023540 (2019), [1905.03254](#).
- [57] M. Adams, F. Bezrukov, J. Elvin-Poole, J. J. Evans, P. Guzowski, B. O. Ferraigh, and S. Söldner-Rembold, *Eur. Phys. J. C* **80**, 758 (2020), [2002.07762](#).
- [58] S. Hagstotz, P. F. de Salas, S. Gariazzo, M. Gerbino, M. Lattanzi, S. Vagnozzi, K. Freese, and S. Pastor, *Phys. Rev. D* **104**, 123524 (2021), [2003.02289](#).
- [59] M. Dentler, A. Hernández-Cabezudo, J. Kopp, P. A. Machado, M. Maltoni, I. Martinez-Soler, and T. Schwetz, *JHEP* **08**, 010 (2018), [1803.10661](#).
- [60] S. Böser, C. Buck, C. Giunti, J. Lesgourgues, L. Ludhova, S. Mertens, A. Schukraft, and M. Wurm, *Prog. Part. Nucl. Phys.* **111**, 103736 (2020), [1906.01739](#).
- [61] A. Serebrov, R. Samoilov, and M. Chaikovskii (2021), [2109.12385](#).
- [62] S. Gariazzo, *J. Phys. Conf. Ser.* **1468**, 012120 (2020), [1911.03463](#).

- [63] S. Gariazzo, C. Giunti, M. Laveder, and Y. F. Li, JHEP **06**, 135 (2017), [1703.00860](#).
- [64] V. Brdar, O. Fischer, and A. Y. Smirnov, Phys. Rev. D **103**, 075008 (2021), [2007.14411](#).
- [65] M. Hostert and M. Pospelov, Phys. Rev. D **104**, 055031 (2021), [2008.11851](#).
- [66] A. Atre, T. Han, S. Pascoli, and B. Zhang, JHEP **05**, 030 (2009), [0901.3589](#).
- [67] D. McKeen and M. Pospelov, Phys. Rev. D **82**, 113018 (2010), [1011.3046](#).
- [68] V. A. Duk et al. (ISTRA+), Phys. Lett. B **710**, 307 (2012), [1110.1610](#).
- [69] M. Drewes and B. Garbrecht, Nucl. Phys. B **921**, 250 (2017), [1502.00477](#).
- [70] A. de Gouvêa and A. Kobach, Phys. Rev. D **93**, 033005 (2016), [1511.00683](#).
- [71] P. Coloma, P. A. Machado, I. Martinez-Soler, and I. M. Shoemaker, Phys. Rev. Lett. **119**, 201804 (2017), [1707.08573](#).
- [72] A. A. Aguilar-Arevalo et al. (MiniBooNE DM), Phys. Rev. D **98**, 112004 (2018), [1807.06137](#).
- [73] J. R. Jordan, Y. Kahn, G. Krnjaic, M. Moschella, and J. Spitz, Phys. Rev. Lett. **122**, 081801 (2019), [1810.07185](#).
- [74] C. A. Argüelles, M. Hostert, and Y.-D. Tsai, Phys. Rev. Lett. **123**, 261801 (2019), [1812.08768](#).
- [75] D. A. Bryman and R. Shrock, Phys. Rev. D **100**, 053006 (2019), [1904.06787](#).
- [76] P. Coloma, Eur. Phys. J. C **79**, 748 (2019), [1906.02106](#).
- [77] D. A. Bryman and R. Shrock, Phys. Rev. D **100**, 073011 (2019), [1909.11198](#).
- [78] A. H. Córscico, L. G. Althaus, M. M. Miller Bertolami, S. O. Kepler, and E. García-Berro, JCAP **08**, 054 (2014), [1406.6034](#).
- [79] S. A. Díaz, K.-P. Schröder, K. Zuber, D. Jack, and E. E. B. Barrios (2019), [1910.10568](#).
- [80] A. Studenikin, in *17th International Conference on Topics in Astroparticle and Underground Physics* (2021), [2111.00469](#).
- [81] A. Radionov, Phys. Rev. D **88**, 015016 (2013), [1303.4587](#).
- [82] M. Antonello et al. (MicroBooNE, LAr1-ND, ICARUS-WA104) (2015), [1503.01520](#).
- [83] A. G. Riess, Nature Rev. Phys. **2**, 10 (2019), [2001.03624](#).
- [84] M. Wyman, D. H. Rudd, R. A. Vanderveld, and W. Hu, Phys. Rev. Lett. **112**, 051302 (2014), [1307.7715](#).
- [85] J. Hamann and J. Hasenkamp, JCAP **10**, 044 (2013), [1308.3255](#).
- [86] G. B. Gelmini, A. Kusenko, and V. Takhistov, JCAP **06**, 002 (2021), [1906.10136](#).
- [87] S. Hannestad, R. S. Hansen, and T. Tram, Phys. Rev. Lett. **112**, 031802 (2014), [1310.5926](#).
- [88] B. Dasgupta and J. Kopp, Phys. Rev. Lett. **112**, 031803 (2014), [1310.6337](#).
- [89] E. W. Kolb and M. S. Turner, Phys. Rev. D **36**, 2895 (1987).
- [90] S. Shalgar, I. Tamborra, and M. Bustamante, Phys. Rev. D **103**, 123008 (2021), [1912.09115](#).
- [91] C. A. Argüelles, K. Farrag, T. Katori, R. Khandelwal, S. Mandalia, and J. Salvado, JCAP **02**, 015 (2020), [1909.05341](#).

- [92] D. F. G. Fiorillo, G. Miele, S. Morisi, and N. Saviano, Phys. Rev. D **101**, 083024 (2020), [2002.10125](#).
- [93] D. F. G. Fiorillo, S. Morisi, G. Miele, and N. Saviano, Phys. Rev. D **102**, 083014 (2020), [2007.07866](#).
- [94] L. Morel, Z. Yao, P. Cladé, and S. Guellati-Khélifa, Nature **588**, 61 (2020).
- [95] G. Bennett et al. (Muon g-2), Phys. Rev. D **73**, 072003 (2006), [hep-ex/0602035](#).
- [96] B. Abi et al. (Muon g-2), Phys. Rev. Lett. **126**, 141801 (2021), [2104.03281](#).
- [97] T. Albahri et al. (Muon g-2), Phys. Rev. D **103**, 072002 (2021), [2104.03247](#).
- [98] K. Shiomi (KOTO), PoS **BEAUTY2020**, 055 (2021).
- [99] A. B. Balantekin, A. de Gouvêa, and B. Kayser, Phys. Lett. B **789**, 488 (2019), [1808.10518](#).
- [100] A. Baha Balantekin and B. Kayser, Ann. Rev. Nucl. Part. Sci. **68**, 313 (2018), [1805.00922](#).
- [101] B. Kayser, in *53rd Rencontres de Moriond on Electroweak Interactions and Unified Theories* (2018), pp. 323–326, [1805.07523](#).
- [102] D. Z. Freedman, Phys. Rev. D **9**, 1389 (1974).
- [103] T. K. Gaisser and J. S. O’Connell, Phys. Rev. D **34**, 822 (1986).
- [104] H.-c. Kim, J. Piekarewicz, and C. J. Horowitz, Phys. Rev. C **51**, 2739 (1995), [nucl-th/9412017](#).
- [105] H.-c. Kim, S. Schramm, and C. J. Horowitz, Phys. Rev. C **53**, 3131 (1996), [nucl-th/9602009](#).
- [106] S. K. Singh and E. Oset, Phys. Rev. C **48**, 1246 (1993).
- [107] J. Engel, E. Kolbe, K. Langanke, and P. Vogel, Phys. Rev. D **48**, 3048 (1993), [nucl-th/9304017](#).
- [108] J. Marteau, J. Delorme, and M. Ericson, Nucl. Instrum. Meth. A **451**, 76 (2000).
- [109] C. Bleve, G. Co, I. De Mitri, P. Bernardini, G. Mancarella, D. Martello, and A. Surdo, Astropart. Phys. **16**, 145 (2001), [nucl-th/0012015](#).
- [110] G. Co’, C. Bleve, I. De Mitri, and D. Martello, Nucl. Phys. B Proc. Suppl. **112**, 210 (2002), [nucl-th/0203025](#).
- [111] P. Vilain et al. (CHARM-II), Phys. Lett. B **335**, 246 (1994).
- [112] E. Valencia et al. (MINERvA), Phys. Rev. D **100**, 092001 (2019), [1906.00111](#).
- [113] D. Perevalov and R. Tayloe (MiniBooNE), AIP Conf. Proc. **1189**, 175 (2009), [0909.4617](#).
- [114] E. Cortina Gil et al. (NA62), JHEP **03**, 058 (2021), [2011.11329](#).
- [115] A. V. Artamonov et al. (BNL-E949), Phys. Rev. D **79**, 092004 (2009), [0903.0030](#).
- [116] M. W. Winkler, Phys. Rev. D **99**, 015018 (2019), [1809.01876](#).
- [117] J. R. Batley et al. (NA48/2), Phys. Lett. B **769**, 67 (2017), [1612.04723](#).
- [118] R. Aaij et al. (LHCb), Phys. Rev. D **95**, 071101 (2017), [1612.07818](#).
- [119] R. Aaij et al. (LHCb), Phys. Rev. Lett. **115**, 161802 (2015), [1508.04094](#).
- [120] J. T. Wei et al. (Belle), Phys. Rev. Lett. **103**, 171801 (2009), [0904.0770](#).

- [121] J. Lees et al. (BaBar), Phys. Rev. Lett. **119**, 131804 (2017), [1702.03327](#).
- [122] G. Mohlabeng, Phys. Rev. D **99**, 115001 (2019), [1902.05075](#).
- [123] M. Duerr, T. Ferber, C. Hearty, F. Kahlhoefer, K. Schmidt-Hoberg, and P. Tunney, JHEP **02**, 039 (2020), [1911.03176](#).
- [124] Y. Kahn, G. Krnjaic, S. Mishra-Sharma, and T. M. P. Tait, JHEP **05**, 002 (2017), [1609.09072](#).
- [125] J. A. Dror, R. Lasenby, and M. Pospelov, Phys. Rev. Lett. **119**, 141803 (2017), [1705.06726](#).
- [126] J. A. Dror, R. Lasenby, and M. Pospelov, Phys. Rev. **D96**, 075036 (2017), [1707.01503](#).